Resonant Conversion of Wave Dark Matter in the Ionosphere

Carl Beadle,[1] Andrea Caputo,[2,3] and Sebastian A. R. Ellis[1]
[1]*Departement de Physique Theorique, Universite de Geneve, 24 quai Ernest Ansermet, 1211 Geneve 4, Switzerland*
[2]*Department of Theoretical Physics, CERN, Esplanade des Particules 1, P.O. Box 1211, Geneva 23, Switzerland*
[3]*Dipartimento di Fisica, "Sapienza" Università di Roma, Italy & Sezione INFN Roma1, Piazzale Aldo Moro 5, 00185, Roma, Italy*

(Received 31 May 2024; revised 24 July 2024; accepted 7 November 2024; published 17 December 2024)

We consider resonant wavelike dark matter conversion into low-frequency radio waves in the Earth's ionosphere. Resonant conversion occurs when the dark matter mass and the plasma frequency coincide, defining a range $m_{\rm DM} \sim 10^{-9}$–10^{-8} eV where this approach is best suited. Owing to the nonrelativistic nature of dark matter and the typical variational scale of the Earth's ionosphere, the standard linearized approach to computing dark matter conversion is not suitable. We therefore solve a second-order boundary-value problem, effectively framing the ionosphere as a driven cavity filled with a positionally varying plasma. An electrically small dipole antenna targeting the generated radio waves can be orders of magnitude more sensitive to dark photon and axionlike particle dark matter in the relevant mass range. This Letter opens up a promising way of testing hitherto unexplored parameter space that could be further improved with a dedicated instrument.

DOI: 10.1103/PhysRevLett.133.251001

Introduction—The nature of dark matter (DM) remains a puzzle that requires an explanation from beyond the standard model (SM) of particle physics. Wavelike dark matter such as an axionlike particle (ALP) or a massive dark photon (DP) are well-motivated candidates [1–10]. Dark photons can naturally have a small coupling to SM photons through kinetic mixing [11], while ALPs can have a CP-odd coupling to two SM photons [12–16]. These two couplings are the subject of intensive theoretical and experimental work [17–21].

A massive DP could arise from an additional $U(1)$ gauge group broken by a compact scalar field, a possibility strongly motivated by UV completions of the SM [22–32]. The small kinetic mixing with the SM photon enables an extensive experimental program to search for DP dark matter (see, e.g., [33] for a summary of ongoing efforts and experimental optimization strategies). UV completions of the SM also often predict the existence of many ALPs [34–37]. These typically couple to photons, with a coupling strength that can be as large as $g_{a\gamma\gamma} \sim 10^{-12}$ GeV^{-1} [38,39].

ALPs are CP-odd pseudoscalars, while DPs are CP-even vectors, making these quite different dark matter candidates. However, they nevertheless often share similar phenomenology. We consider a possible signal due to resonant conversion of wavelike dark matter into radio waves in the Earth's ionosphere that is common to both ALPs and DPs. For the DP signal to exist, the presence of a plasma is sufficient, while for ALPs, a background magnetic field must also be present. Both conditions are met in the weakly ionized plasma of the Earth's ionosphere, where the Earth's small magnetic field ($B \sim 0.1$ G) is present. Nonresonant signatures using the Earth and its ionosphere at lower masses have been studied previously [40–43].

The structure of the interactions between either DPs or ALPs and the SM photon are such that in a medium the mass eigenstates no longer correspond to the vacuum mass eigenstates. When the plasma frequency of the medium and the vacuum mass of the DM are degenerate, resonant level crossing between one state and the other can occur. For DPs, this condition has been exploited to study resonant conversion in various astrophysical environments such as the solar corona [44,45], neutron star magnetospheres [46], or the intergalactic medium [47–50]. For ALPs, this effect has also been studied in many astrophysical environments [51–60].

In this Letter we propose searching for the conversion of dark matter in the Earth's own ionosphere. This approach has two advantageous properties: the ionosphere is well-studied and monitored (see Ref. [61] and references therein), allowing for a precise understanding of the conversion and propagation of the resulting radio waves; the peak plasma frequency in the ionosphere is $\omega_{\rm pl} \sim 10^{-8}$ eV, such that the mass range that can be probed is complementary to existing searches (see Fig. 1). Furthermore, galactic noise is reflected by the ionosphere, such that the dominant noise source is either *anthropogenic* or atmospheric, both of which can be monitored or even partially mitigated. Several features of the ionosphere might allow for an improved ability to distinguish true signals from spurious ones. For example, there is a daily modulation due to solar irradiation varying the free-electron number density, introducing a spectral feature in the true signal that would be absent for certain spurious signals. Finally, for ALP searches, the dependence on the transverse component of the magnetic field makes the amplitude of the signal latitude-dependent. Such variations are the subject of constant monitoring [62], and would have to be accounted for when analyzing collected data.

The idea to resonantly convert dark photons into photons in the Earth's ionosphere was sketched in Ref. [63]. However, Ref. [63] uses an unsuitable approach to estimate the signal, introduced a somewhat arbitrary boost from gravitational focusing to enhance it, and did not conduct an accurate noise analysis, which, as we show, is crucial, and thus did not produce a compelling sensitivity curve. Furthermore, a different measurement technique using a stratospheric balloon was proposed whereas we discuss a ground based antenna. Finally, Ref. [63] did not consider axion conversion.

DM conversion to electromagnetic waves—The DP-photon system is described by the Lagrangian

$$\mathcal{L} \supset -\frac{1}{4}(F_{\mu\nu}F^{\mu\nu} - 2\epsilon F'_{\mu\nu}F^{\mu\nu} + F'_{\mu\nu}F'^{\mu\nu}) + \frac{1}{2}m_{A'}^2 A'_\mu A'^\mu - A_\mu \mathcal{J}^\mu, \quad (1)$$

where primed quantities are associated to the DP, while the axion Lagrangian is

$$\mathcal{L} \supset -\frac{1}{4}\left(F_{\mu\nu}F^{\mu\nu} - 2\partial_\mu a \partial^\mu a + g_{a\gamma\gamma} a F_{\mu\nu}\tilde{F}^{\mu\nu}\right) - \frac{1}{2}m_a^2 a^2 - A_\mu \mathcal{J}^\mu. \quad (2)$$

The parameter ϵ is the kinetic mixing between the photon and the DP, $g_{a\gamma\gamma}$ is the axion-photon coupling, while $m_{A'}$ and m_a are the masses of DPs and axions, respectively. For convenience, we define the effective dark matter-photon coupling $g_{\rm eff} = \epsilon$ for DPs and $g_{\rm eff} = g_{a\gamma\gamma}|\mathbf{B}_T|/m_a$ for axions [64].

The evolution of the photon and dark matter system can be modeled as a two-state system of equations. While in vacuum the photon and dark matter are mass eigenstates, so no mixing can occur, in a medium such as a weakly coupled plasma, the equations of motion of the two states become coupled through their interaction strength $g_{\rm eff}$. The form of the coupled equations implies that as long as $g_{\rm eff}$ is nonzero, resonant two-level crossing can occur when the effective photon mass (i.e., the plasma mass) and the dark matter mass are equivalent. If the spatial variations of the plasma frequency occur on scales much larger than the de Broglie wavelength of the DM [66], then the conversion probability is well-approximated by the Landau-Zener formula [45,69–72]

$$P_{\alpha\to\gamma} \simeq (f_{\rm pol}\pi)\frac{g_{\rm eff}^2 m_\alpha}{v_r}\left|\frac{\partial \ln \omega_{\rm pl}^2}{\partial r}\right|_{r_c}^{-1}, \quad (3)$$

where $\alpha = A', a$ depends on the dark matter candidate being considered. The polarization fraction is $f_{\rm pol} = 2/3, 1$ for the DP and axion, respectively. The probability is evaluated at the conversion radius r_c, where $\omega_{\rm pl}(r_c) = m_\alpha$. The velocity factor $v_r \sim v_0$ is the radial component of the dark matter velocity, with $v_0 \simeq 220$ km/s the galactic dispersion velocity of dark matter [73].

Unfortunately, for the Earth's ionosphere—which we model in what follows using a Chapman profile [74,75] (see the Supplemental Material [76])—and for the dark matter masses of interest, the plasma frequency varies on a scale similar to or smaller than the de Broglie wavelength of the dark matter. As a result, the WKB approximation used in the derivation of the simplified formula in Eq. (3) does not hold, and the full second-order differential equations must be solved. We use the fact that the ionosphere plasma density has a strong gradient only along the z direction to model the problem as a *driven one-dimensional cavity filled with plasma*, where the driver is the DM field. This is a very good approximation due to Snell's law [80]: light rays in the ionosphere naturally experience *strong refraction toward the z direction* as they propagate downward. Therefore, considering only propagation vertical with respect to the ground is good up to corrections that we expect to be suppressed by the ratio $h/R_\oplus \sim 10^{-2}$ (with h being the width of the ionosphere), which sets the difference between the gradients along the parallel and orthogonal directions to the ground.

Thus, the equation to be studied reduces to

$$\left[\partial_z^2 + \omega^2 - \frac{\omega^2\omega_{\rm pl}^2(z)}{\omega^2 + i\nu_c\omega}\right]\mathbf{E}_T(z) = i\omega g_{\rm eff} m_\alpha^2 \mathbf{V}(z), \quad (4)$$

where $\mathbf{E}_T$ is the sourced electric field, $\mathbf{V} = \mathbf{A}'_T(a\hat{\mathbf{B}}_T)$ for the DP (axion), ν_c is the electron-ion collision frequency in the ionosphere, and z is the height into the ionosphere as measured from the Earth's surface. The form of Eq. (4) shows the salient aspects of the problem. When $(\partial_z^2 + \omega^2)\mathbf{E}_T = m_\alpha^2\mathbf{E}_T = \omega_{\rm pl}^2\mathbf{E}_T$, we see that there is a resonance as expected. Meanwhile, when $\omega_{\rm pl}^2 \ll \omega^2$, we obtain the evolution of the transverse electric field as a function of z, subject to the appropriate boundary conditions. For the wavelengths of interest, the Earth acts as a good conductor [40], so that the field should vanish within one skin depth of the surface. Similarly, the plasma of the ionosphere behaves as a conductor for frequencies below $\omega_{\rm pl}$, imposing that the field should also vanish deep inside the plasma. In the above, we are neglecting the effect of the Earth's magnetic field on the motion of the electrons in the plasma. Including it introduces modifications of the equation of motion by the cyclotron frequency, $\Omega_{\rm B} \sim 10^{-9}(B/0.1{\rm Gauss})$ eV. While this frequency is similar to the dark matter masses we consider, we have numerically verified that its impact is limited. Particularly, it does not affect the magnitude of the signal strength. However, for specific dark matter masses (depending on the detector's location), cyclotron motion suppresses one polarization of the signal fields. This effect could possibly aid in detection, so it is important to account for it when analyzing experimental data.

This 1D model breaks down if we consider DM waves with de Broglie wavelengths comparable to the Earth's radius, i.e., for $m_\alpha \lesssim 10^{-10}$ eV. In practice, for DM masses below $m_\alpha \lesssim 10^{-9}$ eV, our model of the ionosphere is a poor approximation of the real data [81], so we restrict ourselves to only considering masses above this value. A technical description of our solution to Eq. (4) is provided in the Supplemental Material. Our formalism automatically takes into account all the wave propagation phenomena, including reflection, absorption, and refraction of the electromagnetic (EM) waves that ultimately arrive at the detector. In fact, because of these propagation effects, the amplitude of the wave at detection point is expected to be different than the amplitude at the resonance point, as we now show.

Figure 2 shows the EM energy density in natural units as a function of the ionosphere height for a fixed effective coupling, $g_{\rm eff} = 10^{-10}$. Different colors correspond to different DM masses; the solid curves are our numerical results, while the horizontal dashed lines show the result of applying Eq. (3). We notice that the resonant peak of each of our curves never deviates too much from the naive calculation. However, the energy density near the Earth's surface, which is the quantity relevant for detection, is typically suppressed with respect to the peak. This is a particularly important effect for large masses, $\sim 10^{-8}$ eV, whose resonant conversion condition is only satisfied for the largest electron densities near the peak of the Chapman profile. An EM wave produced at that height undergoes many reflections as it propagates through the plasma, and its amplitude is therefore attenuated before it reaches the detector. The effect is less evident for smaller masses, where reflection plays only a minor role. The EM energy density near the Earth's surface is approximated to within $\sim 10\%$ by the following sigmoid function:

$$\rho_{\rm EM} \simeq \frac{3\times 10^{-23}\ {\rm eV}^4 (\frac{g_{\rm eff}}{10^{-10}})^2}{1+\exp\left[-\left(\frac{m_\alpha}{2.3\times 10^{-9}\ {\rm eV}} - 3.8\right)\right]}, \tag{5}$$

which is valid for masses in the range $10^{-9} \le m_\alpha/{\rm eV} \lesssim 3\times 10^{-8}$. The lower boundary is defined by the aforementioned issues with the validity of our calculation, while the upper bound is defined by the peak values of the free-electron number density. Ultimately, a detailed analysis taking into account the detector location and time could be performed using real ionosphere data [81], and could extend our sensitivity to smaller masses. We leave this to future work.

Signal detection—The EM radiation incident on the Earth's surface has a characteristic wavelength $\lambda \gg 1$ m, and can therefore be detected with an electrically small antenna [82]. The signal approximated by Eq. (5) is the total integrated energy density. For detection, the more relevant quantity is the spectral density of the EM radiation $\mathcal{S}_{\rm sig}(\omega) \sim \rho_{\rm EM} f(\omega)$. The function $f(\omega)$ is approximately a Maxwell-Boltzmann distribution [73,83], normalized as $\int d\omega f(\omega) = 1$, which describes the frequency dispersion of the signal inherited from the dark matter velocity distribution. The signal is spread between frequencies $\omega \in m_\alpha[1, 1+\sigma^2/2]$, where $\sigma \sim 200$ km/s is the DM dispersion velocity. The bandwidth of the signal is thus narrow, and can be approximated as having an effective quality factor of $Q_{\rm sig} \sim 10^6$. Full details are given in the Supplemental Material.

The dominant noise at the relevant frequencies is from processes external to the receiver antenna. It is primarily a combination of atmospheric and anthropogenic radiation. As a fiducial noise level, we adopt the anthropogenic noise expected at a quiet rural location given by the International Telecommunication Union; see, for example, curve C of Fig. 2 of Ref. [84]. This can be characterized by the characteristic temperature of the Gaussian component of the noise

$$T_{\rm N}(\nu) \simeq 6.1\times 10^7 \left(\frac{\rm MHz}{\nu}\right)^{2.75} {\rm K}. \tag{6}$$

Under the assumption of an equivalent loss-free receiving antenna, this temperature can then be converted to a noise spectral density (see, e.g., Ref. [82] for a pedagogical derivation),

$$\mathcal{S}_{\rm N}(\nu) \simeq \frac{32}{3}\pi^2\nu^2 T_{\rm N}(\nu). \tag{7}$$

A real device might contend not only with this typical anthropogenic noise, but also with impulsive components at particular frequencies. Furthermore, atmospheric noise leads to a temperature that can vary significantly depending on weather conditions, sometimes exceeding typical anthropogenic noise by many orders of magnitude [84].

Both the signal and the noise are external to the antenna, and are filtered by the same transfer function determining the antenna response, which therefore does not enter the signal-to-noise ratio (SNR). As a result, the optimal SNR is given by [67,85]

$${\rm SNR} = \left[t_{\rm int}\int_0^\infty d\nu \left(\frac{\mathcal{S}_{\rm Sig}}{\mathcal{S}_{\rm N}}\right)^2\right]^{1/2}, \tag{8}$$

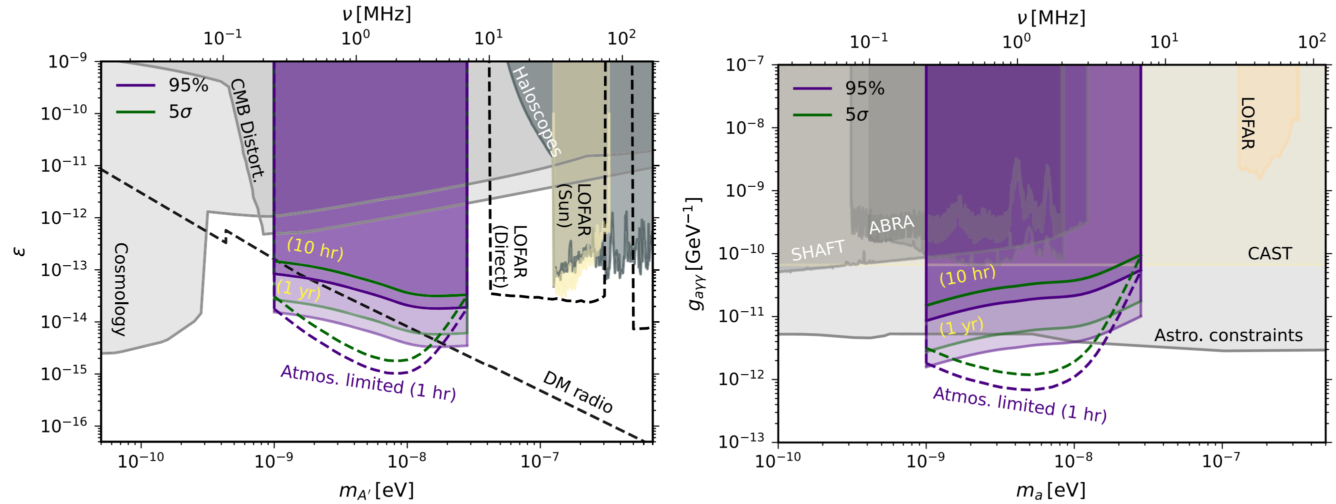

FIG. 1. Left: prospective reach in the DP kinetic mixing ϵ by considering a broadband search with integration time of 10 h and 1 yr (solid curves), for both a 95% (purple) and 5σ (green) discovery potential. The dashed curves indicate the reach of 1 h of observation when measurements are limited by atmospheric noise rather than anthropogenic noise. The light gray region is excluded by cosmological probes [2,49,50], the dark gray region by haloscopes, while the light gold region is excluded by LOFAR observation of the solar corona [45]. The dashed black lines indicate possible future reach of LC-resonator DM radio [93], as well as LOFAR reach for DP *direct* detection in the antenna [97]. Right: projections for the axion to photon coupling $g_{a\gamma\gamma}$, with the same experimental setup used for the DP. The light gray region is excluded by astrophysical probes [88–92], the dark gray regions by terrestrial DM experiments ABRA [94] and SHAFT [95], while the light yellow region is excluded by CAST [96]. The limits from LOFAR observation of the solar corona [45] are shown in light orange.

where $t_{\rm int}$ is the integration time of our measurement (assumed to be larger than the dark matter coherence time). If the receiver antenna is critically coupled, it will have a narrow bandwidth owing to the small radiation resistance. As a result, it is optimal to couple the antenna to an additional in-series resistance. In the Supplemental Material we provide a simple model for an RLC circuit that allows to broaden the frequency response up to $\Delta\nu \sim$ MHz. The circuit we describe, and the value of its parameters, are similar to those of very old radio missions [86,87]. The result of this broad frequency response is that in order to scan an e-fold in DM mass t_e, an integration time at a given frequency of $t_{\rm int} \sim t_e \min(1, 2\pi\Delta\nu/m_\alpha)$ is required.

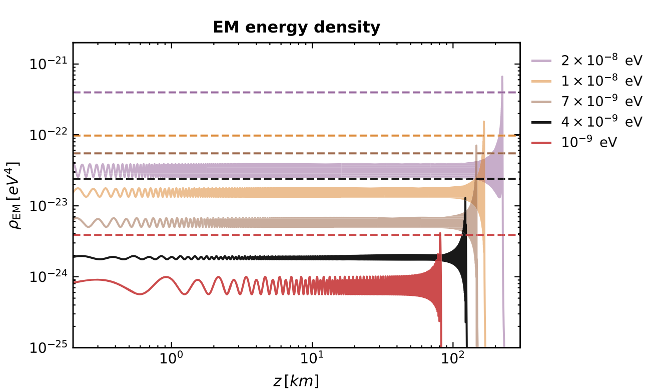

FIG. 2. EM energy density in natural units as a function of the distance z from the Earth surface. Different colors correspond to different DM masses, while the effective coupling is always fixed to $g_{\rm eff} = 10^{-10}$. The solid curves are our full numerical solutions, while the horizontal dashed lines correspond to the Landau-Zener conversion probability from Eq. (3).

Figure 1 shows our fiducial prospects (solid purple lines) for a broadband search with 1 MHz bandwidth, for 10 h and 1 yr of e-fold time, for both DPs (left panel) and axions (right panel). In both panels light gray regions are excluded by cosmological and astrophysical probes [2,49,50,88–92]. Observations by LOFAR of the solar corona are shown in light orange [45] in both panels. For the DP panel the dark gray region is excluded by haloscopes. The dashed black lines indicate possible future sensitivity of DM radio [93], as well as LOFAR sensitivity to *direct* absorption by the antenna. For the axion panel, the dark gray regions are excluded by terrestrial DM experiments ABRA [94] and SHAFT [95], while the light yellow region is excluded by CAST [96].

In case anthropogenic noise can be mitigated, we also show a dashed purple curve corresponding to the typical atmospheric noise in Western Australia around midday on a winter day (see Fig. 18 of Ref. [84]), assuming *a single hour* of e-fold time.

Conclusion—In this Letter we proposed a new way to detect bosonic dark matter with mass $m_\alpha \lesssim 3\times10^{-8}$ eV, i.e., below the typical maximum ionosphere plasma frequency. When DM waves pass through the ionosphere of the Earth, they can get resonantly converted into radio waves that are detectable by a small meter-scale antenna.

Our projections suggest many decades of DP parameter space could be probed in just a few hours of observation time. The small magnetic field of the Earth affects the sensitivity to axions, but we nevertheless project that a similar setup can improve on the best laboratory constraints, and possibly the best astrophysical constraints.

The present work naturally leaves open questions to be addressed in future studies. Fully characterizing the electrical and physical properties of the antenna should be done. The location of the antenna can also be optimized, depending on anthropogenic and atmospheric noise, as well as the Earth's magnetic field for the axion. With a precise detector design and location in mind, a more realistic modeling of the ionosphere plasma frequency using available data [81] can be performed, accounting for diurnal variations. The diurnal variation can be used to look for modulations of our signal, which could be useful in discriminating it from backgrounds. Moreover, our signal can be characterized by the propagation of the signal radially toward the Earth's surface, $\mathbf{k} \propto \hat{\mathbf{r}}$, imprinted by the large plasma gradient in this direction.

Finally, given the simplicity, (small) size, and low cost of the proposed antennas, we envision the use of an array of antennas operating in an interferometric mode. Placing N antennas $\sim\mathcal{O}(10)$ km from each other can improve the signal-to-noise ratio by at least a factor $\sqrt{N}$. The coherence length of the DM signal would exceed the antenna separation, while anthropogenic noise varies more over these scales, thus the potential for improvement is greater if it enables the subtraction of anthropogenic noise sources.

Acknowledgments—We thank Itay Bloch and Sam Witte for multiple enlightening conversations, and Nick Rodd and Kevin Zhou for comments on the manuscript. We particularly thank Pietro Bolli, Giulia Macario, Jader Monari, and Federico Perini for illuminating discussions about low-frequency antennas and radio background noise. The work of C. B. and S. A. R. E. was supported by SNF Ambizione Grant No. PZ00P2_193322, "New frontiers from sub-eV to super-TeV." A. C. is supported by an ERC STG grant ("AstroDarkLS," Grant No. 101117510).

[1] A. E. Nelson and J. Scholtz, Dark Light, dark matter and the misalignment mechanism, Phys. Rev. D **84**, 103501 (2011).

[2] P. Arias, D. Cadamuro, M. Goodsell, J. Jaeckel, J. Redondo, and A. Ringwald, WISPy cold dark matter, J. Cosmol. Astropart. Phys. 06 (2012) 013.

[3] P. W. Graham, J. Mardon, and S. Rajendran, Vector dark matter from inflationary fluctuations, Phys. Rev. D **93**, 103520 (2016).

[4] M. Bastero-Gil, J. Santiago, L. Ubaldi, and R. Vega-Morales, Vector dark matter production at the end of inflation, J. Cosmol. Astropart. Phys. 04 (2019) 015.

[5] R. T. Co, A. Pierce, Z. Zhang, and Y. Zhao, Dark photon dark matter produced by axion oscillations, Phys. Rev. D **99**, 075002 (2019).

[6] J. A. Dror, K. Harigaya, and V. Narayan, Parametric resonance production of ultralight vector dark matter, Phys. Rev. D **99**, 035036 (2019).

[7] P. Agrawal, N. Kitajima, M. Reece, T. Sekiguchi, and F. Takahashi, Relic abundance of dark photon dark matter, Phys. Lett. B **801**, 135136 (2020).

[8] M. Bastero-Gil, J. Santiago, R. Vega-Morales, and L. Ubaldi, Dark photon dark matter from a rolling inflaton, J. Cosmol. Astropart. Phys. 02 (2022) 015.

[9] L. Abbott and P. Sikivie, A cosmological bound on the invisible axion, Phys. Lett. **120B**, 133 (1983).

[10] J. Preskill, M. B. Wise, and F. Wilczek, Cosmology of the invisible axion, Phys. Lett. **120B**, 127 (1983).

[11] B. Holdom, Two U(1)'s and epsilon charge shifts, Phys. Lett. **166B**, 196 (1986).

[12] M. Dine and W. Fischler, The not so harmless axion, Phys. Lett. **120B**, 137 (1983).

[13] M. Dine, W. Fischler, and M. Srednicki, A simple solution to the strong *CP* problem with a harmless axion, Phys. Lett. **104B**, 199 (1981).

[14] J. E. Kim, Weak interaction singlet and strong *CP* invariance, Phys. Rev. Lett. **43**, 103 (1979).

[15] M. A. Shifman, A. I. Vainshtein, and V. I. Zakharov, Can confinement ensure natural *CP* invariance of strong interactions?, Nucl. Phys. **B166**, 493 (1980).

[16] A. R. Zhitnitsky, On possible suppression of the axion hadron interactions. (In Russian), Sov. J. Nucl. Phys. **31**, 260 (1980), https://inspirehep.net/literature/157263.

[17] A. Caputo and G. Raffelt, Astrophysical axion bounds: The 2024 edition, Proc. Sci., COSMICWISPers (2024) 041 [arXiv:2401.13728].

[18] B. R. Safdi, TASI lectures on the particle physics and astrophysics of dark matter, Proc. Sci., TASI2022 (**2024**) 009 [arXiv:2303.02169].

[19] C. A. J. O'Hare, Cosmology of axion dark matter, Proc. Sci., COSMICWISPers (2024) 040 [arXiv:2403.17697].

[20] L. Di Luzio, M. Giannotti, E. Nardi, and L. Visinelli, The landscape of QCD axion models, Phys. Rep. **870**, 1 (2020).

[21] I. G. Irastorza and J. Redondo, New experimental approaches in the search for axion-like particles, Prog. Part. Nucl. Phys. **102**, 89 (2018).

[22] K. R. Dienes, C. F. Kolda, and J. March-Russell, Kinetic mixing and the supersymmetric gauge hierarchy, Nucl. Phys. **B492**, 104 (1997).

[23] J. Giedt, Completion of standard model like embeddings, Ann. Phys. (N.Y.) **289**, 251 (2001).

[24] F. Gmeiner, R. Blumenhagen, G. Honecker, D. Lust, and T. Weigand, One in a billion: MSSM-like D-brane statistics, J. High Energy Phys. 01 (2006) 004.

[25] K. R. Dienes, Statistics on the heterotic landscape: Gauge groups and cosmological constants of four-dimensional heterotic strings, Phys. Rev. D **73**, 106010 (2006).

[26] K. R. Dienes, M. Lennek, D. Senechal, and V. Wasnik, Supersymmetry versus gauge symmetry on the heterotic landscape, Phys. Rev. D **75**, 126005 (2007).

[27] A. Arvanitaki, N. Craig, S. Dimopoulos, S. Dubovsky, and J. March-Russell, String photini at the LHC, Phys. Rev. D **81**, 075018 (2010).
[28] A. Corti, M. Haskins, J. Nordström, and T. Pacini, G_2-manifolds and associative submanifolds via semi-Fano 3-folds, Duke Math. J. **164**, 1971 (2015).
[29] W. Taylor and Y.-N. Wang, A Monte Carlo exploration of threefold base geometries for 4d F-theory vacua, J. High Energy Phys. 01 (2016) 137.
[30] B. S. Acharya, S. A. R. Ellis, G. L. Kane, B. D. Nelson, and M. J. Perry, The lightest visible-sector supersymmetric particle is likely to be unstable, Phys. Rev. Lett. **117**, 181802 (2016).
[31] J. Halverson and P. Langacker, TASI lectures on remnants from the string landscape, Proc. Sci., TASI2017 (**2018**) 019 [arXiv:1801.03503].
[32] B. S. Acharya, A. Maharana, and F. Muia, Hidden sectors in string theory: Kinetic mixings, fifth forces and quintessence, J. High Energy Phys. 03 (2019) 048.
[33] A. Caputo, A. J. Millar, C. A. J. O'Hare, and E. Vitagliano, Dark photon limits: A handbook, Phys. Rev. D **104**, 095029 (2021).
[34] P. Svrcek and E. Witten, Axions in string theory, J. High Energy Phys. 06 (2006) 051.
[35] A. Arvanitaki, S. Dimopoulos, S. Dubovsky, N. Kaloper, and J. March-Russell, String axiverse, Phys. Rev. D **81**, 123530 (2010).
[36] M. Demirtas, N. Gendler, C. Long, L. McAllister, and J. Moritz, PQ axiverse, J. High Energy Phys. 06 (2023) 092.
[37] I. Broeckel, M. Cicoli, A. Maharana, K. Singh, and K. Sinha, Moduli stabilisation and the statistics of axion physics in the landscape, J. High Energy Phys. 08 (2021) 059; 01 (2022) 191(A).
[38] J. Halverson, C. Long, B. Nelson, and G. Salinas, Towards string theory expectations for photon couplings to axionlike particles, Phys. Rev. D **100**, 106010 (2019).
[39] N. Gendler, D. J. E. Marsh, L. McAllister, and J. Moritz, Glimmers from the axiverse, J. Cosmol. Astropart. Phys. 09 (2024) 071.
[40] M. A. Fedderke, P. W. Graham, D. F. Jackson Kimball, and S. Kalia, Earth as a transducer for dark-photon dark-matter detection, Phys. Rev. D **104**, 075023 (2021).
[41] A. Arza, M. A. Fedderke, P. W. Graham, D. F. Jackson Kimball, and S. Kalia, Earth as a transducer for axion dark-matter detection, Phys. Rev. D **105**, 095007 (2022).
[42] M. A. Fedderke, P. W. Graham, D. F. Jackson Kimball, and S. Kalia, Search for dark-photon dark matter in the SuperMAG geomagnetic field dataset, Phys. Rev. D **104**, 095032 (2021).
[43] I. A. Sulai *et al.*, Hunt for magnetic signatures of hidden-photon and axion dark matter in the wilderness, Phys. Rev. D **108**, 096026 (2023).
[44] H. An, F. P. Huang, J. Liu, and W. Xue, Radio-frequency dark photon dark matter across the sun, Phys. Rev. Lett. **126**, 181102 (2021).
[45] H. An, X. Chen, S. Ge, J. Liu, and Y. Luo, Searching for ultralight dark matter conversion in solar corona using LOFAR data, Nat. Commun. **15**, 915 (2024).
[46] E. Hardy and N. Song, Listening for dark photon radio from the galactic centre, Phys. Rev. D **107**, 115035 (2023).
[47] J. S. Bolton, A. Caputo, H. Liu, and M. Viel, Comparison of low-redshift Lyman-α Forest observations to hydrodynamical simulations with dark photon dark matter, Phys. Rev. Lett. **129**, 211102 (2022).
[48] A. Caputo, H. Liu, S. Mishra-Sharma, and J. T. Ruderman, Modeling dark photon oscillations in our inhomogeneous universe, Phys. Rev. D **102**, 103533 (2020).
[49] A. Caputo, H. Liu, S. Mishra-Sharma, and J. T. Ruderman, Dark photon oscillations in our inhomogeneous universe, Phys. Rev. Lett. **125**, 221303 (2020).
[50] S. D. McDermott and S. J. Witte, Cosmological evolution of light dark photon dark matter, Phys. Rev. D **101**, 063030 (2020).
[51] G. Raffelt and L. Stodolsky, Mixing of the photon with low mass particles, Phys. Rev. D **37**, 1237 (1988).
[52] M. S. Pshirkov and S. B. Popov, Conversion of dark matter axions to photons in magnetospheres of neutron stars, J. Exp. Theor. Phys. **108**, 384 (2009).
[53] A. Hook, Y. Kahn, B. R. Safdi, and Z. Sun, Radio signals from axion dark matter conversion in neutron star magnetospheres, Phys. Rev. Lett. **121**, 241102 (2018).
[54] G. Y. Huang, T. Ohlsson, and S. Zhou, Observational constraints on secret neutrino interactions from big bang nucleosynthesis, Phys. Rev. D **97**, 075009 (2018).
[55] S. J. Witte, D. Noordhuis, T. D. P. Edwards, and C. Weniger, Axion-photon conversion in neutron star magnetospheres: The role of the plasma in the Goldreich-Julian model, Phys. Rev. D **104**, 103030 (2021).
[56] J. W. Foster, Y. Kahn, O. Macias, Z. Sun, R. P. Eatough, V. I. Kondratiev, W. M. Peters, C. Weniger, and B. R. Safdi, Green Bank and Effelsberg Radio Telescope searches for axion dark matter conversion in neutron star magnetospheres, Phys. Rev. Lett. **125**, 171301 (2020).
[57] R. A. Battye, B. Garbrecht, J. I. McDonald, F. Pace, and S. Srinivasan, Dark matter axion detection in the radio/mm-waveband, Phys. Rev. D **102**, 023504 (2020).
[58] M. Leroy, M. Chianese, T. D. P. Edwards, and C. Weniger, Radio signal of axion-photon conversion in neutron stars: A ray tracing analysis, Phys. Rev. D **101**, 123003 (2020).
[59] R. A. Battye, J. Darling, J. McDonald, and S. Srinivasan, Towards robust constraints on axion dark matter using psr j1745-2900, 2021, Phys. Rev. D **105**, L021305 (2022).
[60] F. P. Huang, K. Kadota, T. Sekiguchi, and H. Tashiro, Radio telescope search for the resonant conversion of cold dark matter axions from the magnetized astrophysical sources, Phys. Rev. D **97**, 123001 (2018).
[61] M. Materassi, B. Forte, A. J. Coster, and S. Skone, *The Dynamical Ionosphere: A Systems Approach to Ionospheric Irregularity* (Elsevier, New York, 2019).
[62] The Ionosphere Monitoring and Prediction Center, Ionosphere monitoring and prediction, https://impc.dlr.de.
[63] G. Cantatore, S. A. Çetin, H. Fischer, W. Funk, M. Karuza, A. Kryemadhi, M. Maroudas, K. Özbozduman, Y. K. Semertzidis, and K. Zioutas, Dark matter detection in the stratosphere, Symmetry **15**, 1167 (2023).
[64] In this Letter we will take $|\mathbf{B}_T| \sim 0.4$ G and assume it is homogeneous (a good approximation over the scales relevant to the ionosphere) [65].

[65] Magnetic field estimated values, https://www.ngdc.noaa.gov/geomag/calculators/magcalc.shtml#igrfwmm (Accessed: 2024-05-06).

[66] The spatial coherence length of the DM waves is set by its de Broglie wavelength [67]. This is the intuitive reason why this (and not other scales, such as the Compton length) is the important quantity to compare with the density gradient. At the mathematical level, when one studies the equations of motion for the two-level system of interest (photons and DM waves) and passes to Fourier space, it is the *momentum* k_a of the particle that appears in the wave equations to be solved and $1/k_a$ is the quantity to be compared with the plasma characteristic length scale [49,68].

[67] J. W. Foster, N. L. Rodd, and B. R. Safdi, Revealing the dark matter halo with axion direct detection, Phys. Rev. D **97**, 123006 (2018).

[68] N. Brahma, A. Berlin, and K. Schutz, Photon-dark photon conversion with multiple level crossings, Phys. Rev. D **108**, 095045 (2023).

[69] C. Zener, Nonadiabatic crossing of energy levels, Proc. R. Soc. A **137**, 696 (1932).

[70] L. D. Landau, A theory of energy transfer. 2., Phys. Z. Sowjetunion **2** (1932).

[71] S. J. Parke, Nonadiabatic level crossing in resonant neutrino oscillations, Phys. Rev. Lett. **57**, 1275 (1986).

[72] T.-K. Kuo and J. T. Pantaleone, Neutrino oscillations in matter, Rev. Mod. Phys. **61**, 937 (1989).

[73] J. Herzog-Arbeitman, M. Lisanti, and L. Necib, The metal-poor stellar halo in RAVE-TGAS and its implications for the velocity distribution of dark matter, J. Cosmol. Astropart. Phys. 04 (2018) 052.

[74] S. Chapman, The absorption and dissociative or ionizing effect of monochromatic radiation in an atmosphere on a rotating earth part ii. grazing incidence, Proc. Phys. Soc. **43**, 483 (1931).

[75] M. M. Hoque, L. Yuan, F. S. Prol, M. Hernández-Pajares, R. Notarpietro, N. Jakowski, G. Olivares Pulido, A. Von Engeln, and C. Marquardt, A new method of electron density retrieval from metop-as truncated radio occultation measurements, Remote Sens. **15**, 1424 (2023).

[76] See Supplemental Material at http://link.aps.org/supplemental/10.1103/PhysRevLett.133.251001 for extra information on the ionospheric modelling, details on how the signal strength was found and finer points on the proposal to measure the signal. The uncertainties in the sensitivity estimates are also quantified. It includes Refs. [77–79].

[77] S. Chaudhuri, P. W. Graham, K. Irwin, J. Mardon, S. Rajendran, and Y. Zhao, Radio for hidden-photon dark matter detection, Phys. Rev. D **92**, 075012 (2015).

[78] B. T. Draine, *Physics of the Interstellar and Intergalactic Medium* (Princeton University Press, Princeton, 2011).

[79] M. Nicolet, The collision frequency of electrons in the ionosphere, J. Atmos. Terr. Phys. **3**, 200 (1953).

[80] M. Born and E. Wolf, *Principles of Optics* (Cambridge University Press, Cambridge, England, 1999).

[81] C. on Space Research, Iri 2016, https://kauai.ccmc.gsfc.nasa.gov/instantrun/iri.

[82] K. T. McDonald, Power received by a small antenna, http://kirkmcd.princeton.edu/examples/power.pdf.

[83] L. Krauss, J. Moody, F. Wilczek, and D. E. Morris, Calculations for cosmic axion detection, Phys. Rev. Lett. **55**, 1797 (1985).

[84] I. R. Assembly, Radio noise, https://www.itu.int/dms_pubrec/itu-r/rec/p/R-REC-P.372-8-200304-S!!PDF-E.pdf.

[85] S. Chaudhuri, K. Irwin, P. W. Graham, and J. Mardon, Optimal impedance matching and quantum limits of electromagnetic axion and hidden-photon dark matter searches, arXiv:1803.01627.

[86] H. V. Cane, Spectra of the non-thermal radio radiation from the galactic polar regions, Mon. Not. R. Astron. Soc. **189**, 465 (1979).

[87] J. C. Novaco and L. W. Brown, Nonthermal galactic emission below 10 megahertz., Astrophys. J. **221**, 114 (1978).

[88] D. Noordhuis, A. Prabhu, S. J. Witte, A. Y. Chen, F. Cruz, and C. Weniger, Novel constraints on axions produced in pulsar polar cap cascades, Phys. Rev. Lett. **131**, 111004 (2023).

[89] C. Dessert, D. Dunsky, and B. R. Safdi, Upper limit on the axion-photon coupling from magnetic white dwarf polarization, Phys. Rev. D **105**, 103034 (2022).

[90] J. Davies, M. Meyer, and G. Cotter, Constraints on axionlike particles from a combined analysis of three flaring Fermi flat-spectrum radio quasars, Phys. Rev. D **107**, 083027 (2023).

[91] H. Abe *et al.* (MAGIC Collaboration), Constraints on axion-like particles with the perseus galaxy cluster with MAGIC, Phys. Dark Universe **44**, 101425 (2024).

[92] M. Ajello *et al.* (Fermi-LAT Collaboration), Search for spectral irregularities due to photon–axionlike-particle oscillations with the Fermi Large Area Telescope, Phys. Rev. Lett. **116**, 161101 (2016).

[93] S. Chaudhuri, P. W. Graham, K. Irwin, J. Mardon, S. Rajendran, and Y. Zhao, Radio for hidden-photon dark matter detection, Phys. Rev. D **92**, 075012 (2015).

[94] C. P. Salemi, J. W. Foster, J. L. Ouellet, A. Gavin, K. M. W. Pappas, S. Cheng, K. A. Richardson, R. Henning, Y. Kahn, R. Nguyen, N. L. Rodd, B. R. Safdi, and L. Winslow, Search for low-mass axion dark matter with abracadabra-10 cm, Phys. Rev. Lett. **127**, 081801 (2021).

[95] A. V. Gramolin, D. Aybas, D. Johnson, J. Adam, and A. O. Sushkov, Search for axion-like dark matter with ferromagnets, Nat. Phys. **17**, 79 (2020).

[96] V. Anastassopoulos *et al.* (CAST Collaboration), New CAST limit on the axion-photon interaction, Nat. Phys. **13**, 584 (2017).

[97] H. An, S. Ge, W.-Q. Guo, X. Huang, J. Liu, and Z. Lu, Direct detection of dark photon dark matter using radio telescopes, Phys. Rev. Lett. **130**, 181001 (2023).